Geophysical Research Letters

RESEARCH LETTER
10.1029/2019GL083722

Special Section:
The Arctic: An AGU Joint Special Collection

Spatiotemporal Variability of Sea Ice in the Arctic's Last Ice Area

G. W. K. Moore[1,2], A. Schweiger[3], J. Zhang[3], and M. Steele[3]

[1]Department of Physics, University of Toronto, Toronto, Ontario, Canada, [2]Department of Chemical and Physical Sciences, University of Toronto Mississauga, Mississauga, Ontario, Canada, [3]Polar Science Center, Applied Physics Laboratory, University of Washington, Seattle, Washington, USA

Abstract The Arctic Ocean's oldest and thickest sea ice lies along the ~2,000 km arc from the western Canadian Arctic Archipelago to the northern coast of Greenland. Climate models suggest that this region will be the last to lose its perennial ice cover, thus providing an important refuge for ice-dependent species. However, remarkably little is known about the climate or characteristics of the sea ice in this remote and inhospitable region. Here, we use the Pan-Arctic Ice Ocean Modeling and Assimilation System model to show that the ice cover in the region is very dynamic, with changes occurring at a rate twice that of the Arctic Ocean as a whole. However, there are some differences in the changing nature of the ice cover between the eastern and western regions of the Last Ice Area, which include different timing of the annual minimum in ice thickness as well as distinct ice motion patterns associated with ice thickness extrema.

Key Points:
- The Arctic is experiencing a trend towards a smaller, younger, thinner and more mobile ice pack that is expected to continue
- There is interest in the region that will be last to lose its perennial ice cover thus providing a refuge for ice-dependent organisms
- We document the spatiotemporal variability in the sea ice within this region and the associated regional circulation patterns

Supporting Information:
- Supporting information S1

Correspondence to:
G. W. K. Moore,
gwk.moore@utoronto.ca

Citation:
Moore, G. W. K., Schweiger, A., Zhang, J., & Steele, M. (2019). Spatiotemporal variability of sea ice in the arctic's last ice area. *Geophysical Research Letters*, *46*, 11,237–11,243. https://doi.org/10.1029/2019GL083722

Received 17 MAY 2019
Accepted 18 SEP 2019
Accepted article online 15 OCT 2019
Published online 28 OCT 2019

1. Introduction

The continued loss of Arctic sea ice (Stroeve et al., 2012) is cause for concern both as a dramatic indicator of our changing climate (Vihma, 2014) as well as for its impacts on fragile regional ecosystems (Hinzman et al., 2005; Post et al., 2009). In addition to the well-documented reduction in sea ice extent (Parkinson & Cavalieri, 2008), there are also trends toward a thinner (Schweiger et al., 2011), younger (Maslanik et al., 2011), and more mobile (Spreen et al., 2011) Arctic ice pack. These changes have led to stresses on the entire spectrum of ice-dependent organisms from ice algae to polar bears (Lange et al., 2015; Post et al., 2013). Climate models, under various emission scenarios (Sou & Flato, 2009; Wang & Overland, 2012), suggest that these changes will continue, resulting in additional stresses on fragile ice-dependent ecosystems (Barber et al., 2017; Post et al., 2013).

The oldest and thickest sea ice in the arctic is found in an area that extends along the margin of the Arctic Ocean from the Wandel Sea (north of Greenland), southwestward to the Canadian Arctic Archipelago (Bourke & Garrett, 1987; Lindsay & Schweiger, 2015; Maslanik et al., 2011; Melling, 2002; Tilling et al., 2018). Climate models suggest that this region will be the last to lose its perennial ice cover (Laliberté et al., 2016; Sou & Flato, 2009), thus providing an important refuge for ice-dependent species (Folger, 2018; WWF, 2018). As such, knowledge of the climate of this so-called Last Ice Area (LIA) as well as the variability and changing nature of its sea ice are important inputs for decisions regarding the establishment of marine protected sanctuaries (Krajick, 2010; Loewen & Michel, 2018).

For the purposes of this paper, we will refer to the LIA as the region of old and thick ice along the margin of the North American and Greenland Arctic Basins, excluding the channels within the Canadian Arctic Archipelago. In situ observations of ice thickness in this region are limited, with the most comprehensive data coming from declassified submarine under-ice sonar profiles (Bourke & Garrett, 1987; Lindsay & Schweiger, 2015). This data indicated that during the period from the 1960s to the 1970s, mean ice thickness was 5–7 m (Bourke & Garrett, 1987). The presence of the particularly thick ice in the LIA was attributed to ice motion associated with the Beaufort Gyre and the Transpolar Drift (Bourke & Garrett, 1987).

Apart from these general statements, little is known about the processes responsible for the spatiotemporal variability of sea ice within the LIA. Recently, large-scale climate anomalies have been observed to impact sea ice within the LIA, including the early collapse or absence of the Lincoln Sea ice arch at the northern end of Nares Strait (Kwok et al., 2010; Moore & McNeil, 2018), the formation of a previously unrecognized polynya in the Wandel Sea during February 2018 (Ludwig et al., 2019; Moore et al., 2018b), and the

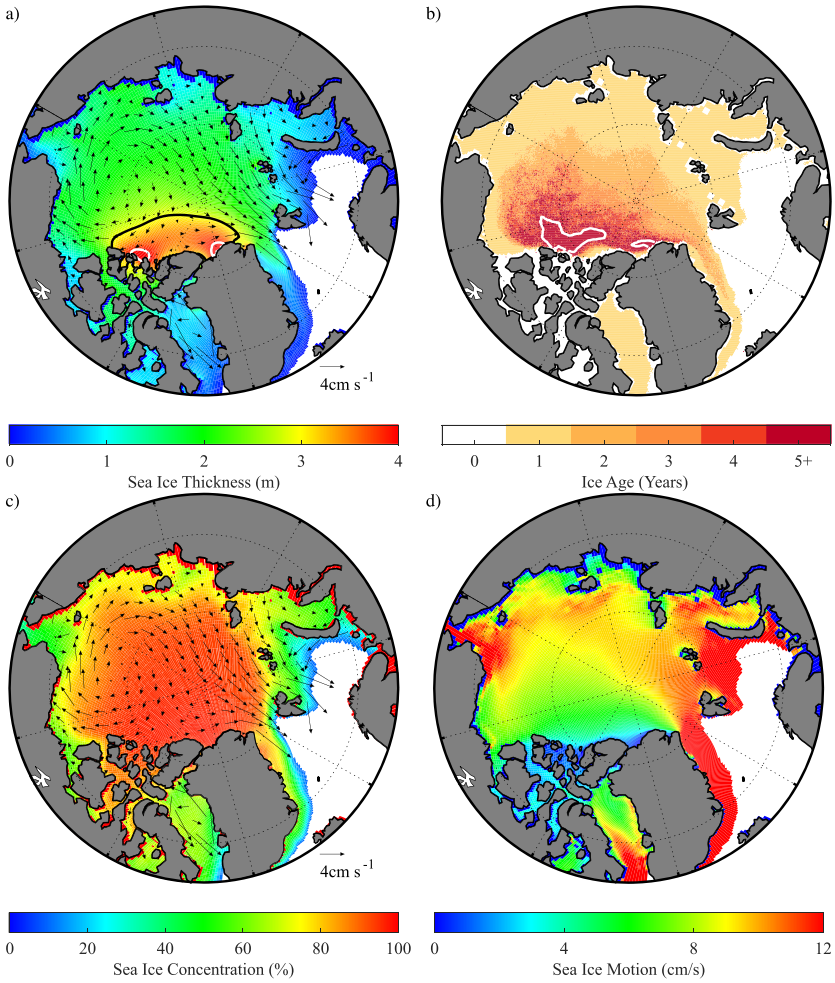

Figure 1. Sea ice: (a) thickness (shading, m) and motion (vectors, cm/s); (b) age (years); (c) concentration (shading, %) and motion (vectors, cm/s); and (d) magnitude of sea ice motion (shading, cm/s). Results in (a), (c), and (d) are annual means from Pan-Arctic Ice Ocean Modeling and Assimilation System, 1979–2018; while results in (b) are April 30 median values from Maslanik et al. (2011), 1984–2017. In (a), the 3 and 4 m thickness isocontour are shown in black and white, respectively. In (b), the white contours encloses areas where the ice age is 5 years or older. Please refer to the Supporting information for details on the coordinates of the 4 m isocontours.

absence of the Beaufort High during the winter of 2017 (Moore et al., 2018a). These results suggest that ice in the region is more dynamic than previously thought (Loewen & Michel, 2018).

Here, we will use output from the Pan-Arctic Ice Ocean Modeling and Assimilation System (PIOMAS, see Supporting information S1 for details) to document the spatiotemporal variability of the sea ice within the LIA. It has undergone extensive validation with a variety of pan-arctic observations, including thickness data (Schweiger et al., 2011; Wang et al., 2016; Zhang & Rothrock, 2003). With respect to the LIA, there is evidence that PIOMAS is unable to represent the thickness gradients that exist as one moves offshore, and as a result, it underrepresents thickness in the region (Schweiger et al., 2011). However, the interannual variability in the PIOMAS sea ice thickness within the LIA is similar to that from CryoSat-2 satellite observations (Ricker et al., 2014; Figure S1).

2. Results

Figure 1 shows the annual mean pan-arctic fields from PIOMAS for the period 1979–2018. The thickest sea ice (thicknesses > 3 m) can be found in the LIA, with two distinct regions where the sea thickness exceeds 4 m, referred to here as the LIA East (LIA-E) and the LIA West (LIA-W; Figure 1a). Please refer to the

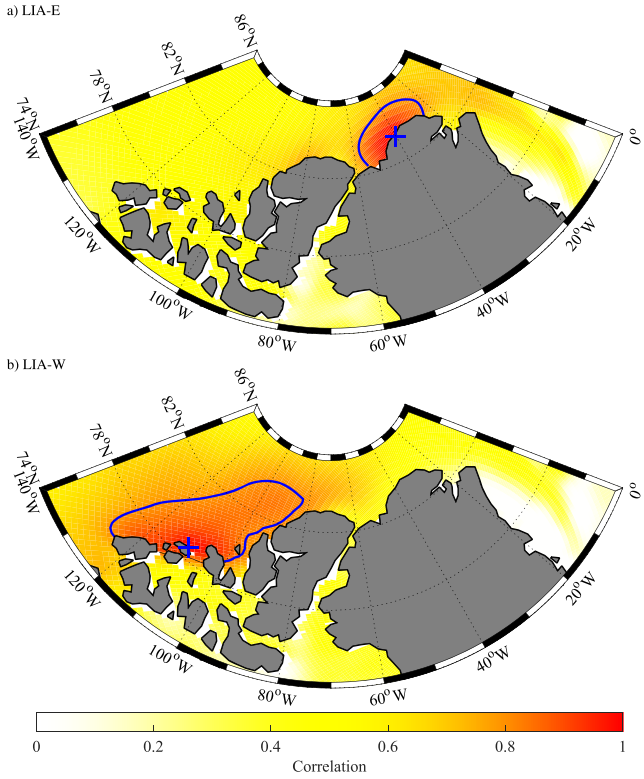

Figure 2. Spatial correlation maps of the annual mean sea ice thickness with time series of annual mean sea ice thickness in the: (a) LIA-E and (b) LIA-W regions. In each case, the 0.8 correlation contour is showing indicating the region where variability in the time series in the respective regions can explain approximately 64% of the variance in the sea ice thickness field. The decorrelation length scale is defined as the median radius from the center point, defined by the "+," to this contour. LIA-E = Last Ice Area East; LIA-W = Last Ice Area West.

Supporting information for details on the boundaries of these two regions. Sea ice age data (Maslanik et al., 2011, Figure 1b) show that these two regions also have the oldest sea ice in the arctic (age > 5 years).

In contrast to the thickness and age data, the annual mean sea ice concentration within the LIA is uniform and close to 100% (Figure 1c). The annual mean sea ice motion field (Figures 1a and 1c) indicates the presence of the anticyclonic Beaufort Gyre and the southeastward motion of the Transpolar Drift (Serreze & Barrett, 2010; Thorndike & Colony, 1982). Annual mean sea ice motion data derived from an independent blend of observations and model output (Tschudi et al., 2016) is consistent with the PIOMAS results (Figure S2). Sea ice speeds within the LIA are low, likely because of relatively thicker and more compact ice of higher mechanical strength (Figure 1d).

Figure 2 indicates that on annual time scales, variability in sea ice thickness between the LIA-E and LIA-W regions is not strongly correlated, providing support for the identification of these regions within the LIA. In particular, the decorrelation length scale (De Benedetti & Moore, 2017), here defined as the median distance over which variability in ice thickness is correlated at the 0.8 level for the locations within the LIA-E and LIA-W regions where the annual mean PIOMAS sea ice thickness is a maximum, indicated by the "+" markers in Figure 2 is ~200 and ~400 km, respectively. To put these distances in context, the distance between these two locations is ~1,300 km.

This result suggests that sea ice variability in the two regions of the LIA should be considered separately. This is done in Figure 3, which shows the time series of the annual mean sea ice thickness, concentration, and ice motion in the two regions. Also shown are the linear trends over the period 1979–2018 as well as a measure of the interannual variability, the detrended standard deviation. All trends are statistically significant at the 99th percentile confidence interval using a test that takes into account the reduced degrees of freedom arising from the temporal autocorrelation of the time series (Moore et al., 2015). Please refer to the Supporting information for details on this significance test. In both regions, sea ice has been thinning at a rate of ~0.4 m/decade, resulting in a thickness loss from the late 1970s of ~1.5 m, a value commensurate with the peak-to-peak interannual variability. Sea ice concentration and ice motion trends and variability differ for the two regions, with LIA-W featuring values approximately twice as large as LIA-E. The corresponding time series for the entire Arctic Ocean north of 70°N (Figure S3) indicate that both the LIA-W and LIA-E are losing ice mass at a rate twice that of the basin average, a result consistent with Bitz and Roe (2004). In contrast, the trend in sea ice concentration loss with the LIA is between 25% and 50% of the basin average. Furthermore, ice speeds within the LIA-W are accelerating at a rate twice that of the basin average, while those in the LIA-E are accelerating at ~50% of the basin average.

To assess temporal changes in sea ice characteristics, the annual cycles of sea ice thickness, concentration, and motion in the two regions within the LIA are shown in Figure 4 for the first, 1979–1998, and second, 1999–2018, halves of the period of interest as well as the difference between the two halves. Sea ice in the two regions tends to be thinner, lower in concentration, and more mobile in late summer and early fall (July–September) as compared to the late winter and early spring (March–May). Over the period of interest, there is a divergence in the timing of the extrema in sea ice thickness between the two regions (Figures 4a and 4b). In particular, the minimum in the LIA-W is tending to occur earlier in the season. The reason for this behavior can be seen in the difference in the seasonal cycle of sea ice thickness between the two periods. For the LIA-W, this difference is largest during August at 1.3 m. To put this value in context, the mean difference in thickness over all the months was 0.8 m, with a standard deviation of 0.2 m; thus the August difference exceeded the mean difference by over two standard deviations. This difference is more uniformly distributed throughout the year in the LIA-E. In contrast to the ice thickness results, the reduction in sea

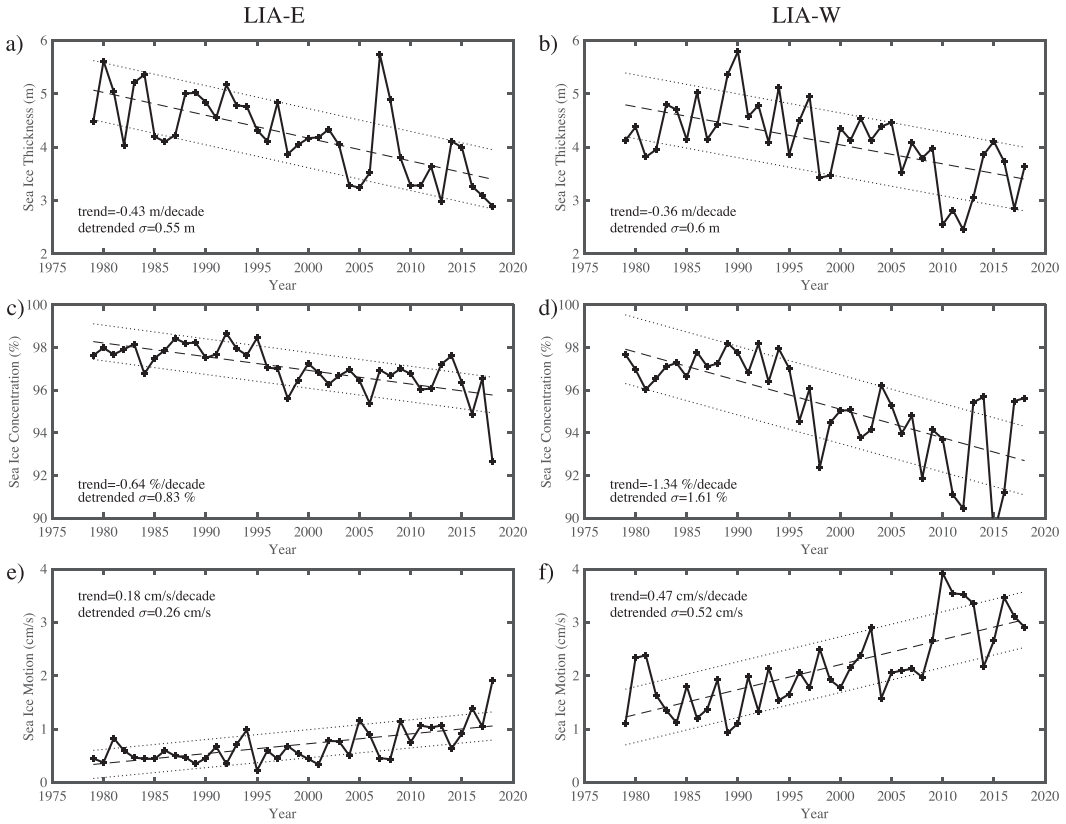

Figure 3. Time series of annual mean sea ice: (a) thickness (m), (b) concentration (%), and (c) motion (cm/s) in the LIA-E region from Pan-Arctic Ice Ocean Modeling and Assimilation System, 1979–2018. Time series of annual mean sea ice: (b) thickness (m), (d) concentration (%), and (f) motion (cm/s) in the LIA-W region from Pan-Arctic Ice Ocean Modeling and Assimilation System, 1979–2018. For each time series, the linear trend is also shown as a dashed line with one detrended standard deviation above and below the linear trend indicated by the dotted lines. LIA-E = Last Ice Area East; LIA-W = Last Ice Area West.

ice concentration tends to be more focused during the summer period with minima occurring approximately 1 month earlier that that for sea ice thickness (Figures 4c and 4d) In addition, the timing of the maximum ice speed in both regions is occurring earlier in the season, with marked increase in sea ice mobility in the LIA-W that is not seen in the LIA-E (Figures 4e and 4f).

As noted above, there is considerable interannual variability in the annual mean sea ice thickness in the LIA-E and LIA-W regions. To investigate the environmental conditions responsible for this variability, the detrended annual mean sea ice thickness time series in the two regions were used to generate spatial correlation maps with the detrended annual mean sea ice thickness and two components of the sea ice motion (Figure 5). For both regions, a bimodal signature in the sea ice thickness correlations is seen, with positive values in the LIA and negative values along the Siberian coast. For the LIA-E region, the correlations show that ice thicknesses variability in this region is associated with transport across the Arctic, southeastward in years with high thicknesses that would tend to advect ice towards this region (Figure 5a). Similarly, high thickness in the LIA-W is also associated with southeastward motion, which is associated with a cyclonic anomaly in this instance, which would also tend to advect ice towards this region (Figure 5b).

To further explore the meteorological controls on these spatially coherent structures, the correlation between the detrended ice thickness time series from the two regions and the principal components of the three leading empirical orthogonal functions (EOFs) of the annual mean sea-level pressure field north of 60°N were computed (Overland & Wang, 2010) using the ERA-I reanalysis (Dee et al., 2011). The leading EOF represents the arctic oscillation (AO) (Thompson & Wallace, 1998), while the second and third represent the arctic dipole (Wu et al., 2006) and the Barents oscillation (BO; Skeie, 2000), respectively. The AO has been

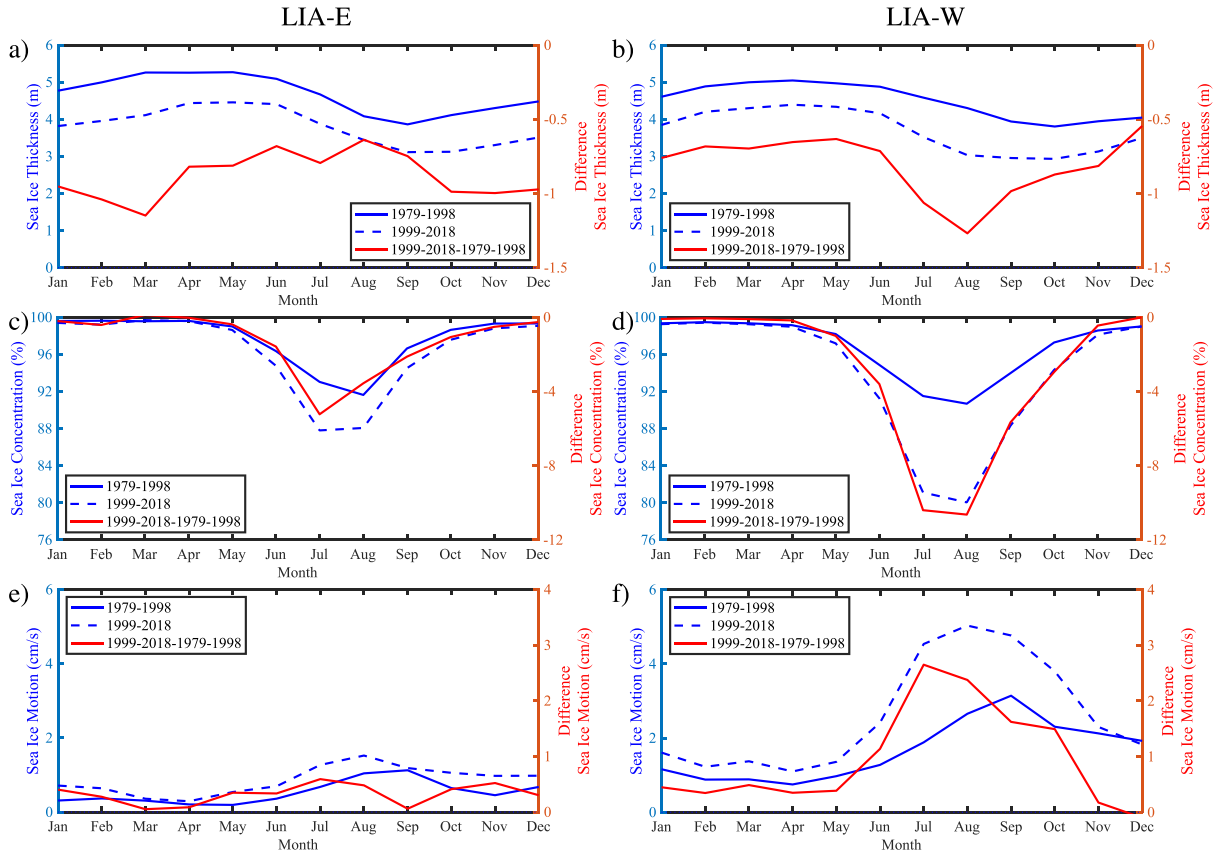

Figure 4. The annual cycle in sea ice: (a) thickness (m), (b) concentration (%), and (c) motion (cm/s) in the LIA-E region from Pan-Arctic Ice Ocean Modeling and Assimilation System. The annual cycle in sea ice: (b) thickness (m), (d) concentration (%), and (e) motion (cm/s) in the LIA-W region from Pan-Arctic Ice Ocean Modeling and Assimilation System. In all cases, the annual cycles over 1979–1998 and 1999–2018 are indicated by the blue solid and dashed curves, respectively. The difference between the two periods is indicated by the red curves. LIA-E = Last Ice Area East; LIA-W = Last Ice Area West.

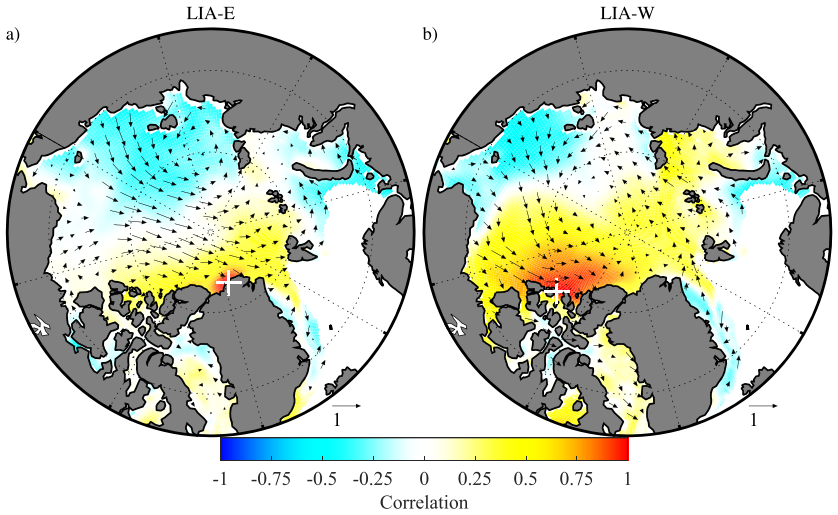

Figure 5. Correlation maps of the annual mean sea ice thickness (shading) and ice motion (vectors) with the detrended time series of annual ice thickness anomalies in the (a) LIA-E and (b) LIA-W regions. The respective regions of interest, LIA-E and LIA-W, are indicated by the "+". LIA-E = Last Ice Area East; LIA-W = Last Ice Area West.

shown to drive gyre-like sea ice motion within the Arctic Ocean (Rigor et al., 2002),while ice motion associated with the Transpolar Drift and export through Fram Strait have been shown to be associated with both the arctic dipole and BO (Skeie, 2000; Wu et al., 2006). With respect to the LIA-E, the correlation coefficients with the three principal components are 0.38, 0.20, and 0.24 and so the circulation anomalies associated with all three EOFs contribute to the interannual variability in sea ice thickness. In the LIA-W, the three principal components have correlation coefficients of 0.57, 0.04, and 0.16, and so it is primarily the AO with a smaller contribution from the BO that contribute to the interannual variability of sea ice thickness in this region.

3. Discussion

The results presented in this paper indicate that there is considerable temporal variability in the sea ice characteristics within the LIA. First and foremost, sea ice within the LIA is highly dynamic, with a peak-to-peak seasonal amplitude in thickness of 1.2 m, a value of the same order as the loss in thickness that has occurred since 1979. This result implies that the LIA is losing ice mass at twice the rate seen in the Arctic Ocean as a whole.

Although the ice in the LIA is much thicker than other areas of the Arctic Ocean, a closer examination reveals two distinct subregions with different dynamics and seasonal and interannual variability. For the purposes of this paper, the two subregions, the LIA-E and LIA-W, were defined by the 4-m annual mean ice thickness contours. However, the decorrelation length scale analysis suggests that results would be unchanged with other similar definitions of these subregions. These new results suggests that contrary to current thinking (Folger, 2018; Loewen & Michel, 2018), it may be a simplification to consider the LIA as being a homogeneous region and that it is important to consider regional variability in sea ice characteristics. This finding has a variety of implications, for example, for the planning of marine refuges in the region (Ferreira, 2019; Wright, 2019).

We also found basin-scale coherent patterns in ice motion associated with extrema in ice thickness in the LIA-E and LIA-W that are related to variability in the leading modes of atmospheric variability within the Arctic, namely, the AO, the dipole anomaly, and the BO (Overland & Wang, 2010). With respect to the LIA-E, extrema in ice thickness was found to be associated with transport across the arctic that would tend to advect sea ice into the region during years with high ice thicknesses, with the opposite happening in low ice thickness years. For the LIA-W, the ice thickness extrema are associated with a gyre-like circulation in the western arctic that would also act to advect ice into the region during high ice thickness years and out of the region during low ice thickness years.

Given the relationship between ice thickness variability within the LIA with pan-arctic ice motion and atmospheric circulation anomalies, the future evolution of sea ice within the LIA, and by association the health of ice dependent ecosystems, may be impacted by changes in these large scale circulation patterns, which arise as the arctic continues to warm (Fyfe et al., 1999).

Acknowledgments
PIOMAS data are available from the Polar Sciences Center at the University of Washington, the ice age and ice motion data are available from the NSIDC. The CryoSat-2 data are available from Helmholtz Centre for Polar and Marine Research of the Alfred Wegener Institute. G. W. K. M. would like to acknowledge funding from the Natural Sciences and Engineering Research Council of Canada. A. S. was supported by ONR grant N00014-17-1-3162, NSF grant OPP-1744587, and NOAA grant NA15OAR4310162. J. Z. was supported by NASA grants NNX17AD27G and NNX15AG68G, NSF grant PLR-1603259, and NOAA grant NA15OAR4310170. M. S. was supported by NASA grant NNX16AK43G, NOAA grant NA15OAR4320063, NSF grants PLR-1503298 and OPP-1751363, and ONR grant N00014-17-1-2545.

References

Barber, D. G., Meier, W. N., Gerland, S., Mundy, C. J., Holland, M., Kern, S., et al. (2017). Arctic sea ice. In *Snow, Water, Ice and Permafrost in the Arctic (SWIPA) 2017*. Oslo, Norway: Arctic Monitoring and Assessment Programme (AMAP).

Bitz, C. M., & Roe, G. H. (2004).A mechanism for the high rate of sea ice thinning in the Arctic Ocean. *Journal of Climate*, *17*(18), 3623–3632. https://doi.org/10.1175/1520-0442(2004)017<3623:Amfthr>2.0.Co;2

Bourke, R. H., & Garrett, R. P. (1987). Sea ice thickness distribution in the Arctic Ocean. *Cold Regions Science and Technology*, *13*(3), 259–280. https://doi.org/10.1016/0165-232X(87)90007-3

De Benedetti, M., & Moore, G. W. K. (2017). Impact of resolution on the representation of precipitation variability associated with the ITCZ. *Geophysical Research Letters*, *44*, 12,519–512,526. https://doi.org/10.1002/2017GL075714

Dee, D. P., Uppala, S. M., Simmons, A. J., Berrisford, P., Poli, P., Kobayashi, S., et al. (2011). The ERA-interim reanalysis: Configuration and performance of the data assimilation system. *Quarterly Journal of the Royal Meteorological Society*, *137*(656), 553–597. https://doi.org/10.1002/qj.828

Ferreira, B. (2019). Saving the Arctic's "Last Ice Area" is a race against time. Retrieved from https://www.vice.com/en_us/article/pa7ym7/saving-the-arctics-last-ice-area-is-a-race-against-time

Folger, T. (2018). Here's where the arctic's wildlife will make its last stand. *The National Geographic Magazine*

Fyfe, J. C., Boer, G. J., & Flato, G. M. (1999). The Arctic and Antarctic oscillations and their projected changes under global warming. *Geophysical Research Letters*, *26*(11), 1601–1604. https://doi.org/10.1029/1999GL900317

Hinzman, L. D., Bettez, N. D., Bolton, W. R., Chapin, F. S., Dyurgerov, M. B., Fastie, C. L., et al. (2005). Evidence and implications of recent climate change in northern Alaska and other arctic regions. *Climatic Change*, *72*(3), 251–298.

Krajick, K. (2010). The last arctic sea ice refuge. Retrieved from https://blogs.ei.columbia.edu/2010/12/17/the-last-arctic-sea-ice-refuge/

Kwok, R., Toudal Pedersen, L., Gudmandsen, P., & Pang, S. S. (2010). Large sea ice outflow into the Nares Strait in 2007. *Geophysical Research Letters*, *37*, L03502. https://doi.org/10.1029/2009GL041872

Laliberté, F., Howell, S. E. L., & Kushner, P. J. (2016). Regional variability of a projected sea ice-free Arctic during the summer months. *Geophysical Research Letters*, *43*, 256–263. https://doi.org/10.1002/2015GL066855

Lange, B. A., Michel, C., Beckers, J. F., Casey, J. A., Flores, H., Hatam, I., et al. (2015). Comparing springtime ice-algal chlorophyll a and physical properties of multi-year and first-year sea ice from the Lincoln Sea. *PLoS ONE*, *10*(4), e0122418. https://doi.org/10.1371/journal.pone.0122418

Lindsay, R., & Schweiger, A. (2015). Arctic sea ice thickness loss determined using subsurface, aircraft, and satellite observations. *The Cryosphere*, *9*(1), 269–283. https://doi.org/10.5194/tc-9-269-2015

Loewen, T. N., & Michel, C. (2018). Proceedings of the multidisciplinary arctic program (MAP)—last ice: Science planning workshop, January 16-17, 2018.

Ludwig, V., Spreen, G., Haas, C., Istomina, L., Kauker, F., & Murashkin, D. (2019). The 2018 North Greenland polynya observed by a newly introduced merged optical and passive microwave sea-ice concentration dataset. *The Cryosphere*, *13*(7), 2051–2073.

Maslanik, J., Stroeve, J., Fowler, C., & Emery, W. (2011). Distribution and trends in Arctic sea ice age through spring 2011. *Geophysical Research Letters*, *38*, L13502. https://doi.org/10.1029/2011GL047735

Melling, H. (2002). Sea ice of the northern Canadian Arctic Archipelago. *Journal of Geophysical Research*, *107*(C11), 3181. https://doi.org/10.1029/2001JC001102

Moore, G. W. K., & McNeil, K. (2018). The early collapse of the 2017 Lincoln Sea ice arch in response to anomalous sea ice and wind forcing. *Geophysical Research Letters*, *45*, 8343–8351. https://doi.org/10.1029/2018GL078428

Moore, G. W. K., Schweiger, A., Zhang, J., & Steele, M. (2018a). Collapse of the 2017 winter Beaufort High: A response to thinning sea ice? *Geophysical Research Letters*, *45*, 2860–2869. https://doi.org/10.1002/2017GL076446

Moore, G. W. K., Schweiger, A., Zhang, J., & Steele, M. (2018b). What caused the remarkable February 2018 North Greenland polynya? *Geophysical Research Letters*, *45*, 13,342–13,350. https://doi.org/10.1029/2018GL080902

Moore, G. W. K., Våge, K., Pickart, R. S., & Renfrew, I. A. (2015). Decreasing intensity of open-ocean convection in the Greenland and Iceland seas. *Nature Climate Change*, *5*(9), 877–882.

Overland, J. E., & Wang, M. (2010). Large-scale atmospheric circulation changes are associated with the recent loss of arctic sea ice. *Tellus A: Dynamic Meteorology and Oceanography*, *62*(1), 1–9. https://doi.org/10.1111/j.1600-0870.2009.00421.x

Parkinson, C. L., & Cavalieri, D. J. (2008). Arctic sea ice variability and trends, 1979-2006. *Journal of Geophysical Research*, *113*, C07003. https://doi.org/10.1029/2007JC004558

Post, E., Bhatt, U. S., Bitz, C. M., Brodie, J. F., Fulton, T. L., Hebblewhite, M., et al. (2013). Ecological consequences of sea-ice decline. *Science*, *341*(6145), 519.

Post, E., Forchhammer, M. C., Bret-Harte, M. S., Callaghan, T. V., Christensen, T. R., Elberling, B., et al. (2009). Ecological dynamics across the arctic associated with recent climate change. *Science*, *325*(5946), 1355.

Ricker, R., Hendricks, S., Helm, V., Skourup, H., & Davidson, M. (2014). Sensitivity of CryoSat-2 arctic sea-ice freeboard and thickness on radar-waveform interpretation. *The Cryosphere*, *8*(4), 1607–1622. https://doi.org/10.5194/tc-8-1607-2014

Rigor, I. G., Wallace, J. M., & Colony, R. L. (2002). Response of sea ice to the arctic oscillation. *Journal of Climate*, *15*(18), 2648–2663.

Schweiger, A., Lindsay, R., Zhang, J., Steele, M., Stern, H., & Kwok, R. (2011). Uncertainty in modeled arctic sea ice volume. *Journal of Geophysical Research*, *116*, C00D06. https://doi.org/10.1029/2011JC007084

Serreze, M. C., & Barrett, A. P. (2010). Characteristics of the Beaufort sea high. *Journal of Climate*, *24*(1), 159–182. https://doi.org/10.1175/2010JCLI3636.1

Skeie, P. (2000). Meridional flow variability over the Nordic Seas in the arctic oscillation framework. *Geophysical Research Letters*, *27*(16), 2569–2572. https://doi.org/10.1029/2000GL011529

Sou, T., & Flato, G. (2009). Sea ice in the Canadian Arctic Archipelago: Modeling the past (1950–2004) and the future (2041–2060). *Journal of Climate*, *22*(8), 2181–2198. https://doi.org/10.1175/2008JCLI2335.1

Spreen, G., Kwok, R., & Menemenlis, D. (2011). Trends in arctic sea ice drift and role of wind forcing: 1992–2009. *Geophysical Research Letters*, *38*, L19501. https://doi.org/10.1029/2011GL048970

Stroeve, J. C., Serreze, M. C., Holland, M. M., Kay, J. E., Malanik, J., & Barrett, A. P. (2012). The arctic's rapidly shrinking sea ice cover: A research synthesis. *Climatic Change*, *110*(3), 1005–1027. https://doi.org/10.1007/s10584-011-0101-1

Thompson, D. W., & Wallace, J. M. (1998). The arctic oscillation signature in the wintertime geopotential height and temperature fields. *Geophysical Research Letters*, *25*(9), 1297–1300.

Thorndike, A. S., & Colony, R. (1982). Sea ice motion in response to geostrophic winds. *Journal of Geophysical Research*, *87*(C8), 5845–5852. https://doi.org/10.1029/JC087iC08p05845

Tilling, R. L., Ridout, A., & Shepherd, A. (2018). Estimating arctic sea ice thickness and volume using CryoSat-2 radar altimeter data. *Advances in Space Research*, *62*(6), 1203–1225. https://doi.org/10.1016/j.asr.2017.10.051

Tschudi, M., Fowler, C., Maslanik, J., Stewart, J., & Meier, W. (2016). Polar pathfinder daily 25 km EASE-grid sea ice motion vectors, version 3. *National Snow and Ice Data Center Distributed Active Archive Center, accessed February*.

Vihma, T. (2014). Effects of arctic sea ice decline on weather and climate: A review. *Surveys in Geophysics*, *35*(5), 1175–1214. https://doi.org/10.1007/s10712-014-9284-0

Wang, M., & Overland, J. E. (2012). A sea ice free summer arctic within 30 years: An update from CMIP5 models. *Geophysical Research Letters*, *39*, L18501. https://doi.org/10.1029/2012GL052868

Wang, X., Key, J., Kwok, R., & Zhang, J. (2016). Comparison of Arctic sea ice thickness from satellites, aircraft, and PIOMAS data. *Remote Sensing*, *8*(9), 713.

Wright, T. (2019). Trudeau seeks to highlight climate policy in visit to Canada's far north. Globe and Mail. Retrieved from https://www.theglobeandmail.com/politics/article-trudeau-seeks-to-highlight-climate-policy-in-visit-to-canadas-far/

Wu, B., Wang, J., & Walsh, J. E. (2006). Dipole anomaly in the winter arctic atmosphere and its association with sea ice motion. *Journal of Climate*, *19*(2), 210–225.

WWF (2018). Last Ice Area. Retrieved from http://www.wwf.ca/conservation/arctic/lia/

Zhang, J., & Rothrock, D. A. (2003). Modeling global sea ice with a thickness and enthalpy distribution model in generalized curvilinear coordinates. *Monthly Weather Review*, *131*(5), 845–861. https://doi.org/10.1175/1520-0493(2003)131<0845:MGSIWA>2.0.CO;2